International Journal of Research in Engineering, Science and Management
Volume 4, Issue 6, June 2021
https://www.ijresm.com | ISSN (Online): 2581-5792

Power Flow Control in Hybrid Microgrids

Ragipani Sribhargavi[1*], A. Raghuram[2]
[1]*M. Tech. Student, Department of Electrical and Electronics Engineering, JNTUH College of Engineering, Hyderabad, India*
[2]*Professor, Department of Electrical and Electronics Engineering, JNTUH College of Engineering, Hyderabad, India*

***Abstract*: Power management in a hybrid structure is proposed in this paper. A DC microgrid and an AC grid are in this hybrid structure. Due to the technology advancement, the use of a DC micro-grid is increasing. The demand for a DC microgrid is growing as the number of micro sources grows. The total system's efficiency and reliability are improved by employing a hybrid structure. A back to back (B2B) converter is used to connect the DC microgrid and the AC grid. The suggested design allows the DC microgrid to function alone or in conjunction with the AC grid. The power management technique employs several ac-dc-ac conversions. A novel intelligent controller is designed to control the power flow amongst different sources distributed throughout the two types of sub grids, enabling them to share the load more effectively. Overall hybrid grid performance and individual sub grid performance is verified with Matlab simulations.**

***Keywords*: Power management, microgrid, back to back converter, voltage source converter, MPPT control, photo voltaic, wind turbine model.**

1. Introduction

Harvesting energy from renewable energy sources (RESs) is required in future power systems mainly due to the environmental concerns and sustainability [1]. The elevated invasion of renewable resources like wind and solar energy has made them a smart option for designing modern power systems. Despite several advantages coming with the use of RESs, there are many challenges that need to be addressed in order to incorporate them into the utility grid. Some of the main challenges regarding this are reliability and robustness, controllability, and cost-effectiveness. In order to overcome these challenges and utilize distributed RESs more efficiently, MGs are used as building blocks of the future power generation systems. The hybrid structure power system is required at distribution side.

DC (Direct Current) distribution networks are more appropriate for the adoption of distributed energy to create energy internet [2] compared to AC distribution networks, without issues such as three-phase imbalance, synchronization. The key trend for the potential growth of DC power grids [2,3] is the emergence of new energy grid integration. DC Micro grid can be used by proposed hybrid structure. In the proposed scheme, DC micro grid can be conveniently interlinked to AC Grid [4]. In this structure, PV panels, batteries and corresponding DC load is present. This forms islanded DC micro-grid. This type of structure is beneficial in the hilly areas where the transmission lines cannot reach.

A new droop control scheme is proposed for AC and DC micro grid in [5]. Voltage source converter (VSC) is used for interlinking distributed generator [6, 7] with utility grid.

Medium Voltage (MV) islanded micro-grid Active Power Regulation is mentioned in [8]. This system is of considerable benefit where improved transient response is necessary. The hybrid micro-grid and its idea of power sharing are also proposed in [9].

This paper describes the design and study of the hybrid micro grids control scheme. DC microgrid and AC grid are connected with a back to back converter. A solar PV, wind and regulated BESS with a bidirectional buck boost converter are included in the DC microgrid. The microgrid is designed for autonomous operation and the sources are connected to converters to provide the grid with electricity. The back to back converter connects a load of 5 KW to the grid. To minimize the ripple content at the output of the converter, an additional LC filter is used. In MATLAB-Simulink, the simulation model is performed with the control objective of performing the device at a stable point, subjected to different generation and load operating conditions. The simulation is performed to check the stability of the microgrid with adjustments in PV irradiance, wind speed and load. The simulation is also performed to check the load reliability with ac grid or dc microgrid alone & ac grid & dc microgrid combined.

2. System Structure

In this project, the system structure is considered is in Fig. 1. This system has AC grid, DC micro-grid connected by back to back (B2B) converter. The AC grid have AC supply connected to utility load.

AC grids are built by synchronizing two or more networks t ogether. AC grid must remain intact when there would be no solar energy for efficient power generation. The renewable sources along with BESS are connected to the DC bus, which maintains a constant bus voltage of 330 Volts. The key source of electricity in DC microgrid is from solar PV and wind. With the help of the boost converter operated at MPPT, the voltage from the PV is boosted and sent to the DC grid, likewise, the wind voltage did pass via MPPT and then to the DC grid. The PMSG based wind turbine model is connected to the DC bus with a diode rectifier and a boost converter for MPPT operation.

*Corresponding author: bhargaviragipani@gmail.com

The changes in output power lead by the changes in wind speed, holds the bus voltage unchanged. A boost converter is used to link the solar PV array to the grid. The load capacity attached to the micro grid is 5 KW. The battery is a type of Nickel-Cadmium with the capacity of 200volts and 6.5Ah. The battery's chemical characteristic does not take into account as more necessary is electrical characteristic. PV panel provides time-dependent output; it is collected in the battery. State of charging decides the battery behaviour. It is possible to use the charge controller to maintain the fixed output at PV panel, wind and battery.

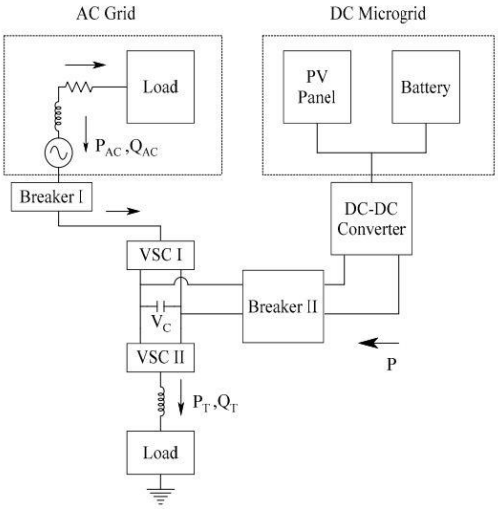

Fig. 1. System Structure for power management

At B2B connection, DC micro grid and the AC grid are interlinked by B2B converter. There are two voltage sourced converters (VSC) in B2B converter. Across VSC I, DC output voltage is obtained. VSC I and VSC II are used to provide back-to-back connection.

In this structure,

1. B2B converter is used to obtain isolation between AC grid and DC micro-grid.
2. Management of power between AC grid and DC micro-grid can be done.
3. At faulty condition, islanded operation is possible.

Interface of DC micro-grid and AC grid can be seen in this structure, i.e. utility grid. P_{ac}&Q_{ac} are the active & reactive power from utility. DC systems output is P_{dcn} (of n^{th} DG).

3. Modelling and Control Strategy

A. Solar PV Modelling and MPPT

A simple single diode model shown in Fig. 2 is considered.

The resistors R_{sh} & R_s are shunt and series resistors. The value of R_{sh} is high about 550Ω as compared to R_s is low about 0.055Ω. The series resistance reflects the contact resistance of PV cell elements while the parallel resistance models the P-N junction's leakage current.

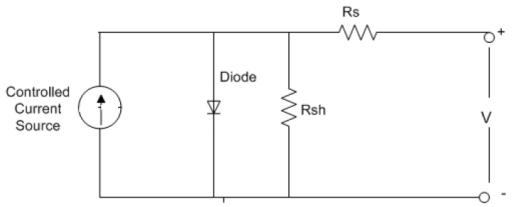

Fig. 2. Single diode PV model

The PV cell's DC current is represented as,

$$I = I_{PV,CELL} - I_{S,CELL}\left(e^{\frac{V}{aVt}} - 1\right) \quad (1)$$

Where,

$I_{PV,CELL}$ is current of PV cell, proportional to intensity of irradiance

$I_{S,CELL}$ is current of diode, expresses the nonlinear relationship between the current and voltage of PV cell

Commercial photovoltaic modules are available as series sets and/or parallel-connected PV cells combined into one component, the PV module, to generate higher voltage, power and current. Boost converter is used in this paper to step up operating voltage at maximum power point [10]. The DC-DC power converter connects the solar panel to the load.

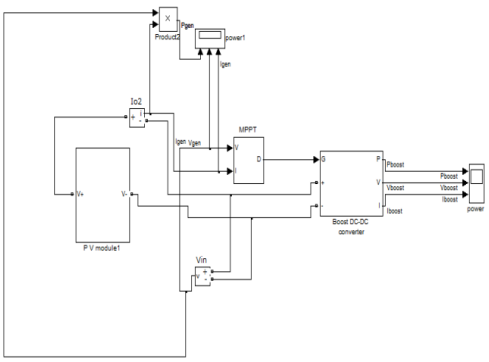

Fig. 3. Complete SIMULINK model of Boost Converter model of MPPT

The core of the model is the MPPT block which helps to locate the solar panel's maximum operating point. It is possible through the use of MPPT algorithms [11]. That in turn gives Boost converter gating signal that maintains the operating voltage at the maximum operating point regardless of solar irradiance and temperature. In this paper, Perturb & Observe MPPT algorithm is used. The complete SIMULINK model of the proposed work is as shown in Fig. 3.

B. Modelling of Wind and MPPT

Wind energy system converts Kinetic Energy of mass (m), air density (ρ), velocity of wind (v) into electrical energy. The block diagram of wind energy system is given in Fig. 4.

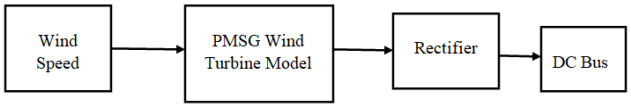

Fig. 4. Block diagram of a Wind Energy System

The wind power captured by wind turbine is expressed as,

$$p = \frac{1}{2} C_p(\lambda, \beta) \rho \pi R^2 V^3 \quad (4)$$

Where,

$Cp\ (\lambda, \beta)$ is the coefficient of wind turbine power that is a function of λ and β

ρ is density of air (kg/m^3)

R is wind turbine blade radius (m)

V is the wind speed (m/s)

β is pitch angle of blade (deg)

λ is speed ratio of tip

$$\lambda = \frac{\omega R}{V} \quad (5)$$

Where,

w is the rotational speed of wind turbine.

In this project, the HCS MPPT algorithm is used to regulate wind power generation operation at Maximum Power Point [12]. The HCS algorithm for implementation of MPPT control logic for wind power generation is shown in Fig. 5. Controller inputs are PMSG voltage, current, and speed.

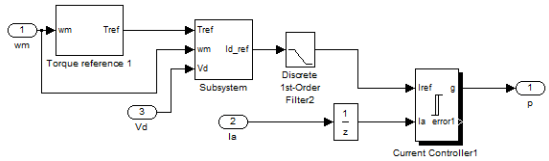

Fig. 5. Sub-system implementation of MPPT control for Wind Power system

C. *Modelling of storage power system*

A generic battery model suitable for dynamic simulation is considered in this work as described in [13]. In this model, Nickel Metal Hydride battery is used with nominal voltage of 200V and 6.5Ah capacity. PI battery control unit is used for charging and discharging in order to maintain DC grid voltage. This model assumes that the battery consists of a controlled-voltage source and series resistance, as shown in Fig. 6. The SOC is considered by this generic battery model as the only state variable.

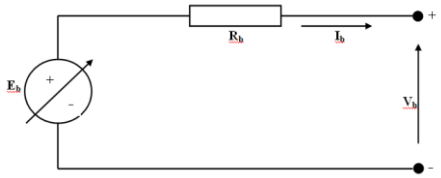

Fig. 6. A generic battery model

The controlled voltage source is given by the following expression,

$$E = E_O - \frac{V_P Q_b}{Q_b - \int i_b dt} + \hat{A} exp(-B_t \int i_b dt) \quad (6)$$

Where,

E is no load voltage

E_o is the constant voltage of battery (V)

V_p is the polarization voltage (V)

Q_b is the battery capacity (AH)

i_b is the battery current (A)

$\hat{A}$ is amplitude of exponential zone (V)

B is inverse of exponential zone time constant (AK')

4. Results and Discussions

In Simulink, the simulation model was built using distinct components from the Simulink library. The model's input source is solar PV and wind also with battery as an energy storage device and a 5KW output load. The machine is simulated for a 5 second period. Initially, in this project, to understand the stability of DC micro grid; various operating conditions are performed by varying wind speed & solar irradiation. They are:

1. Solar irradiation and Wind speed increases and decreases
2. Solar irradiation decreases and Wind speed increases
3. Solar irradiation increases and Wind speed decreases
4. Solar irradiation is variable and Wind speed is constant
5. Solar irradiation is constant and Wind speed is variable

After the constant voltage of DC micro grid is examined, the simulation is performed under various operating conditions for effective and efficient transmission, power management examination. They are:

1. Fixed power from DC micro-grid and AC grid
2. Fixed power from AC grid
3. Fixed power from DC micro-grid

A. *Solar irradiation and Wind speed increases and decreases*

The simulation is carried out with variable solar irradiation and wind speed. The pattern of solar irradiation and wind speed is increased initially and later decreased. The various input solar irradiation given to the PV Module are 600W/m^2, 700W/m^2, 800W/m^2, 1000W/m^2, 900W/m^2 and the input speeds given to the wind turbine model are 0m/s, 5m/s, 7m/s, 12m/s, 10m/s for 1sec to 5 sec respectively. The apparent load is maintained at 5220VA (5kW & 1500VAR).

Equivalent simulink models for variable solar irradiation and variable wind speed are shown in below Fig. 7 and Fig. 8 respectively.

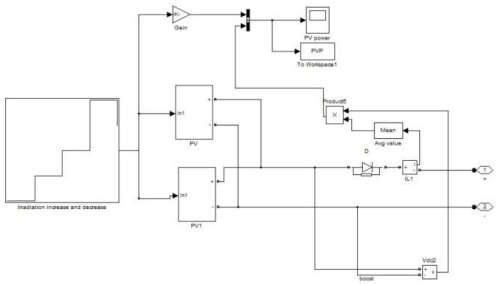

Fig. 7. Equivalent simulink model for variable solar irradiation

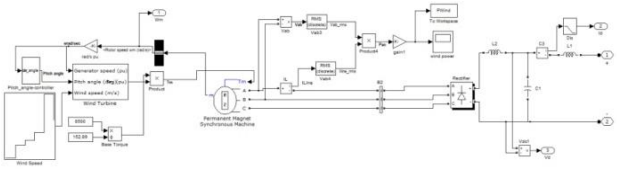

Fig. 8. Equivalent simulink model for variable wind speed

The simulation results shows how solar output power, wind output power changes to the variable solar irradiation & Wind speeds. As the solar output power depends on the irradiation directly, when the irradiation is increased, solar output power is increased. In the end, when the irradiation is decreased, solar output power also decreased. Solar output power values are approximately 5000W, 6000W, 7000W, 9000W and 8000W respectively for 1sec to 5sec.

Similarly, as the wind speed is increased and decreased, wind output power also increased initially and later decreased. Wind output power values approximately are 500W, 1000W, 5000W and 4000W respectively for 1sec to 5sec. This can be observed in Fig. 9 & Fig. 10 respectively. Also, change in SOC of battery, battery power has also been plotted in Fig. 11 & Fig. 12 respectively. It can be observed that, as the battery is in charging, SOC is increasing & the battery power is in negative.

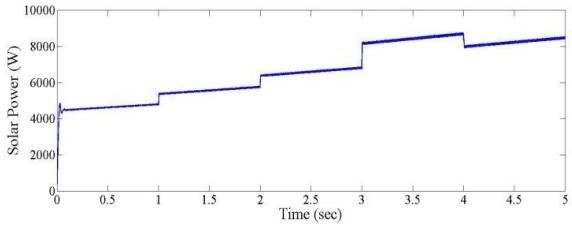

Fig. 9. Solar power when the irradiation is increased and decreased

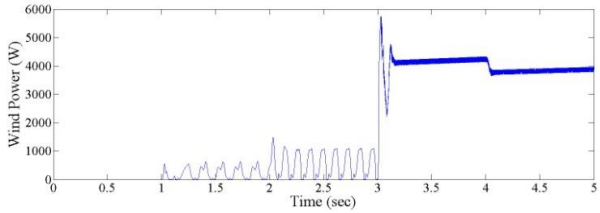

Fig. 10. Wind Power when the wind speed increased and late decreased

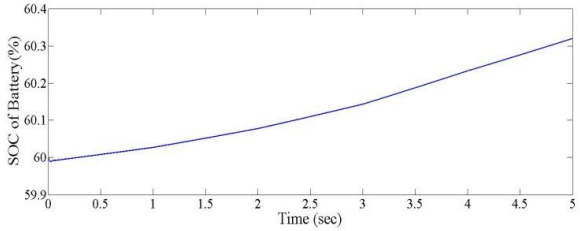

Fig. 11. SOC of Battery when both solar irradiation and wind speed increased and decreased

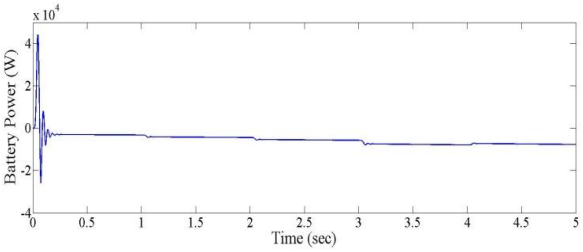

Fig. 12. Battery Power when both solar irradiation and wind speed increased and decreased

B. Solar irradiation decreases and wind speed increases

The simulation is carried out by descending order of solar irradiation and ascending order of wind speed. The various input solar irradiation given to the PV Module are 1000W/m^2, 900W/m^2, 800W/m^2, 700W/m^2, 600W/m^2 and the input speeds given to the wind turbine model are 0m/s, 5m/s, 7m/s, 10m/s, 12m/s for 1sec to 5 sec respectively. The apparent load is maintained at 5220VA (5kW & 1500VAR).

Equivalent simulink models for decrease in solar irradiation and increase in wind speed is shown in below Fig. 13 and Fig. 14 respectively.

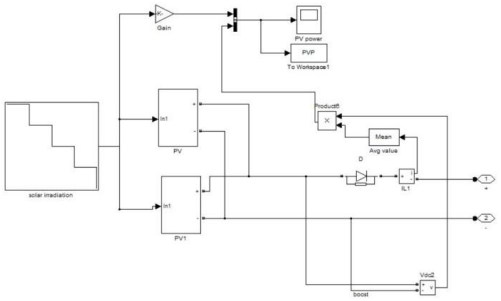

Fig. 13. Equivalent simulink model for decrease in solar irradiation

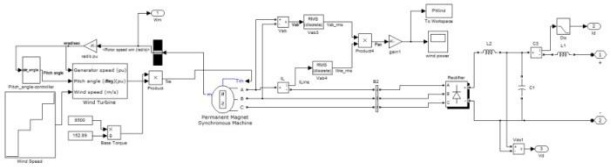

Fig. 14. Equivalent simulink model for increase in wind speed

The simulation results shows how solar output power, wind output power changes to the variable solar irradiation & Wind speeds. As the solar irradiation is decreased, solar output power is decreased with the values 7000W, 6800W, 6000W, 5000W, 4800W approximately. Similar to it, as the wind speed is increased, wind output power also increased with the values 0W, 500W, 1000W, 4000W, 5000W approximately. This can be observed in Fig. 15 & Fig. 16 respectively. Also, change in SOC of battery, battery power has also been plotted in Fig. 17 & Fig. 18 respectively. It can be observed that, as the battery is in charging, SOC is increasing & the battery power is in negative.

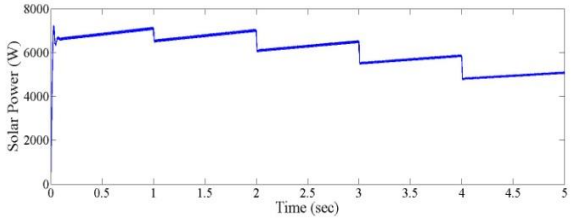

Fig. 15. Solar power when irradiation decreases

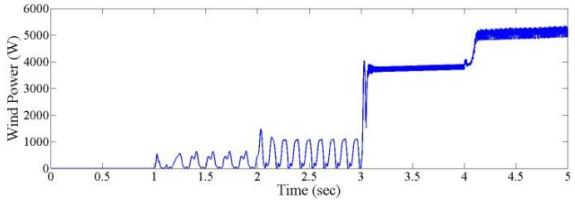

Fig. 16. Wind power when wind speed increases

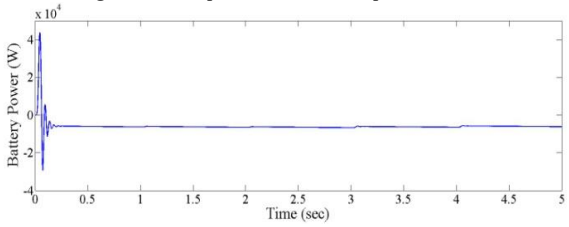

Fig. 17. Battery power when irradiation decreases and wind speed increases

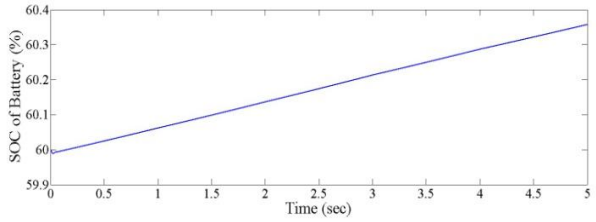

Fig. 18. SOC of Battery when solar irradiation decreases and wind speed increases

C. Solar irradiation increases and wind speed decreases

The simulation is carried out by ascending order of solar irradiation and descending order of wind speed. The various input solar irradiation given to the PV Module are 600W/m^2, 700W/m^2, 800W/m^2, 900W/m^2, 1000W/m^2 and the input speeds given to the wind turbine model are 0m/s, 12m/s, 10m/s, 7m/s, 5m/s, for 1sec to 5 sec respectively. The apparent load is maintained at 5220VA (5kW & 1500VAR).

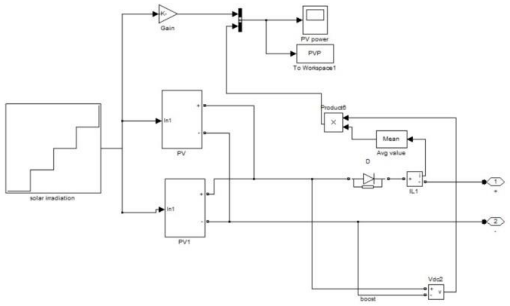

Fig. 19. Equivalent simulink model for increase in solar irradiation

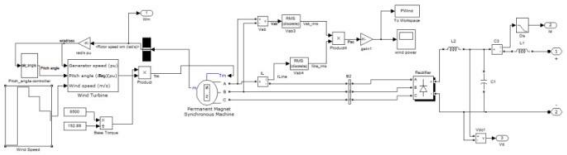

Fig. 20. Equivalent simulink model for decrease in wind speed

Equivalent simulink models for increase in solar irradiation and decrease in wind speed are shown in Fig. 19 and Fig. 20 respectively.

The simulation results shows how solar output power, wind output power changes to the variable solar irradiation & Wind speeds. As the solar irradiation is increased, solar output power is increased approximately with the values 5000W, 6000W, 7000W, 8000W, 9000W. Similar to it, as the wind speed is decreased, wind output power also decreased corresponding to it with the values 5000W, 4000W, 3500W, 3000W approximately for 2sec to 5 sec. This can be observed in Fig. 21 and Fig. 22 respectively. Also, change in SOC of battery, battery power has also been plotted in Fig. 23 and Fig. 24 respectively. It can be observed that, as the battery is in charging, SOC is increasing and the battery power is in negative.

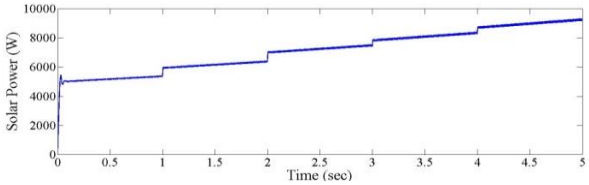

Fig. 21. Solar power when irradiation increases

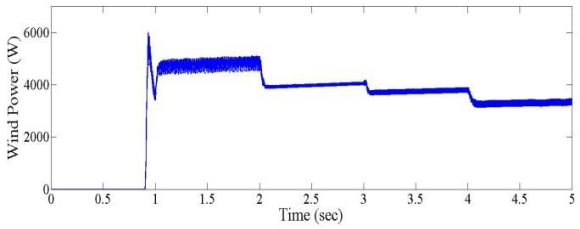

Fig. 22. Wind power when wind speed decreases

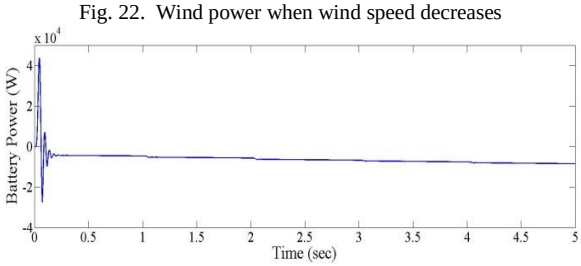

Fig. 23. Battery Power when solar irradiation decreases and wind speed increases

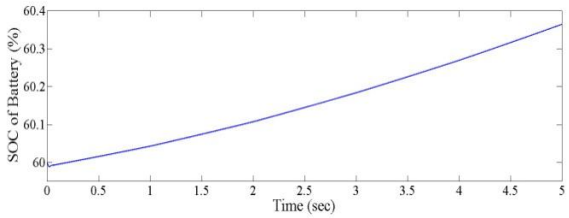

Fig. 24. SOC of Battery when solar irradiation decreases and wind speed increases

D. Solar irradiation is variable and wind speed is constant

The simulation is carried out by variable solar irradiation and constant wind speed. The various input solar irradiation given to the PV Module are 600W/m^2, 700W/m^2, 800W/m^2, 1000W/m^2, 900W/m^2 and the input speeds given to the wind turbine model are 0m/s, 12m/s, 12m/s, 12m/s, 12m/s, for 1sec to 5 sec respectively. The apparent load is maintained at 5220VA (5kW & 1500VAR).

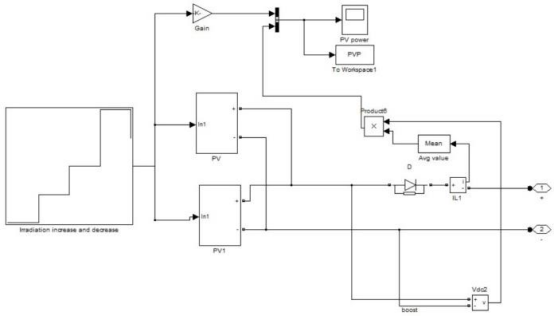

Fig. 25. Equivalent simulink model for variable solar irradiation

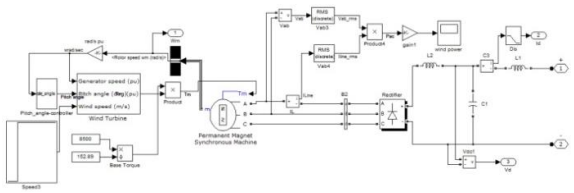

Fig. 26. Equivalent simulink model for constant wind speed

Equivalent simulink models for variable solar irradiation and constant wind speed are shown in Fig. 25 and Fig. 26 respectively.

The simulation results shows how solar output power, wind output power changes to the variable solar irradiation & constant wind speed. As the solar irradiation is varied, solar output power values are 5000W, 6000W, 7000W, 8000W, 7000W. Similar to it, for constant wind speed, wind output power values are 3500W, 3500W, 3500W and 3500W approximately for 2sec to 5 sec. This can be observed in Fig. 27 & Fig. 28 respectively. Also, change in SOC of battery, battery power has also been plotted in Fig. 29 & Fig. 30 respectively. It can be observed that, as the battery is in charging, SOC is increasing & the battery power is in negative.

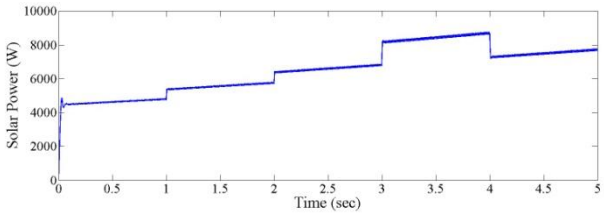

Fig. 27. Solar power for variable solar irradiation

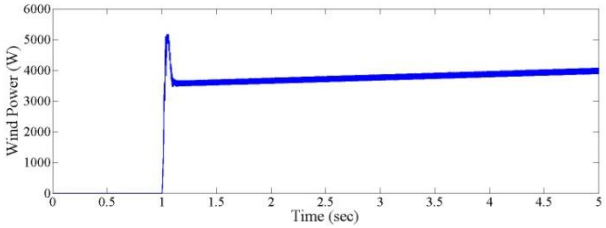

Fig. 28. Wind power for constant wind speed

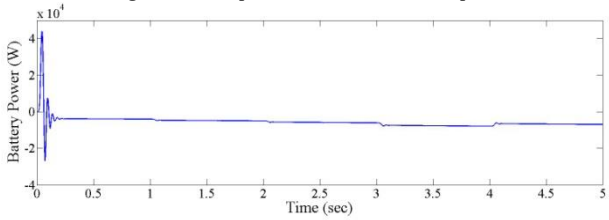

Fig. 29. Battery Power for variable solar irradiation and constant wind speed

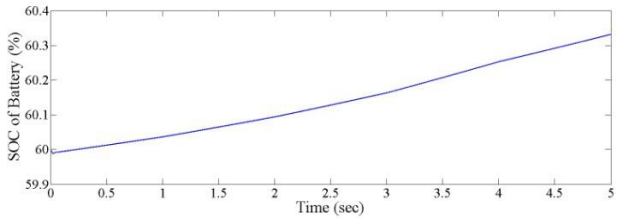

Fig. 30. SOC of Battery for variable solar irradiation and constant wind speed

E. Solar irradiation is constant and wind speed is variable

The simulation is carried out by constant solar irradiation and variable wind speed. The various input solar irradiation given to the PV Module are 1000W/m^2, 1000W/m^2, 1000W/m^2, 1000W/m^2, 1000W/m^2 and the input speeds given to the wind turbine model are 0m/s, 5m/s, 7m/s, 12m/s, 10m/s, for 1sec to 5 sec respectively. The apparent load is maintained at 5220VA (5kW & 1500VAR).

Equivalent simulink models for variable solar irradiation and constant wind speed are shown in Fig. 31 and Fig. 32 respectively.

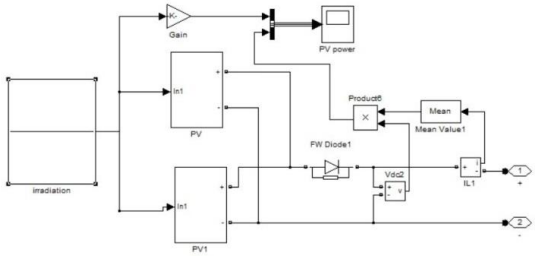

Fig. 31. Equivalent simulink model for constant solar irradiation

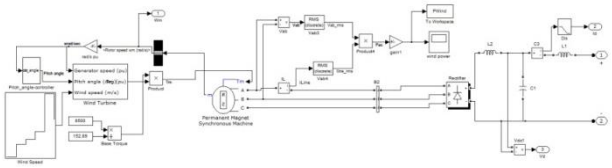

Fig. 32. Equivalent simulink model for variable wind speed

The simulation results shows how solar output power, wind output power changes to the constant solar irradiation & variable wind speed. As the solar irradiation is varied, solar output power values are 7000W, 7500W, 8000W, 8500W, 9000W. Similar to it, for variable wind speed, wind output power values are 500W, 1000W, 5000W and 4000W approximately for 2sec to 5 sec. This can be observed in Fig. 33 & Fig. 34 respectively. Also, change in SOC of battery, battery power has also been plotted in Fig. 35 & Fig. 36 respectively. It can be observed that, as the battery is in charging, SOC is increasing & the battery power is in negative.

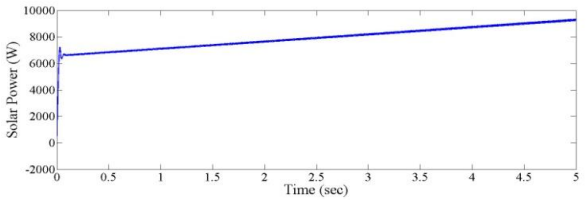

Fig. 33. Solar Power for constant solar irradiation

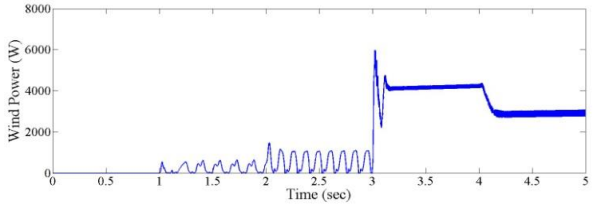

Fig. 34. Wind Power for variable wind speed

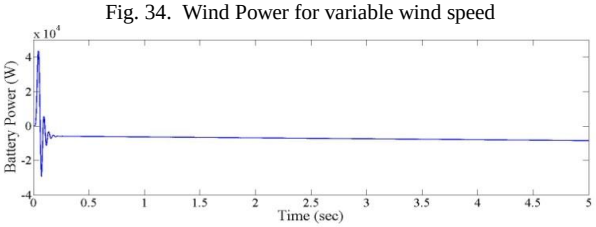

Fig. 35. Battery Power for constant solar irradiation and variable wind speed

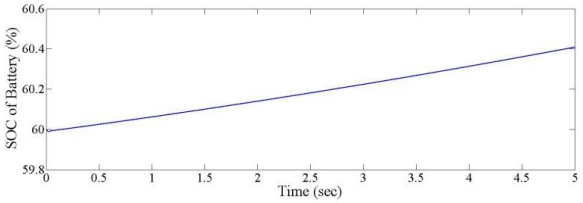

Fig. 36. SOC of Battery for constant solar irradiation and variable wind speed

In these operating modes, the effects of the simulation are checked under the excess power mode and deficit power mode and the control of BESS. The effect of these changes on DC micro grid is observed. For all the above cases, DC Bus voltage is shown in Fig. 37. By this, the suggested model also demonstrates that under all its operating conditions, the system retains a constant DC bus voltage at 330V DC. We can consider that DC Micro grid is stable for all these conditions.

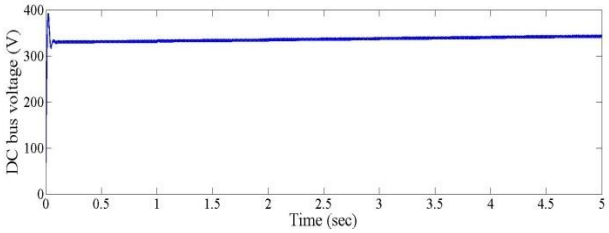

Fig. 37. DC Bus Voltage for all the operating modes

Let us observe the following 3 cases for power management between AC grid & DC Micro grid.

F. Fixed power from dc micro-grid and ac grid

For this case, solar irradiation is maintained constant at 1000W/m^2 and wind speed is maintained constant at 12m/s. The apparent load is maintained at 5220VA (5kW, 1500VAR).

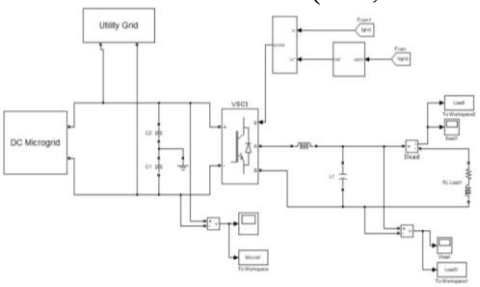

Fig. 38. Equivalent simulink model for fixed power from DC micro grid and AC grid

Results of these changes are observed. Equivalent simulink model for fixed power from DC micro grid and AC grid is shown in Fig. 38.

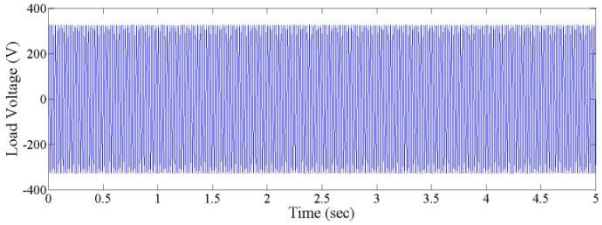

Fig. 39. Output Voltage for fixed power from AC grid & DC micro grid

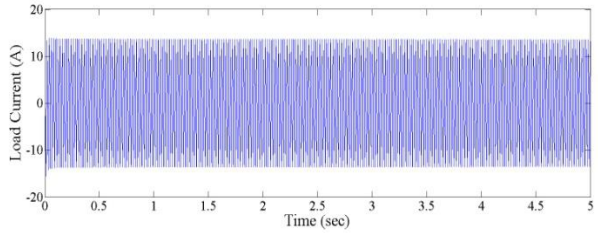

Fig. 40. Output Current for fixed power from AC grid & DC micro grid

The simulation scheme for this case is shown in the Fig. 1. In this case, power from both AC grid and DC grid is combined and given to load of 5KW. The output response for this case is shown in the Fig. 39 & Fig. 40

Observation:

The condition is healthy, i.e. no fault at any network. The output response includes both AC grid and DC micro grid inputs. In this case, voltage and current observed are 220V rms and 7.63A rms. The voltage output is regulated via B2B converter. The response indicated here is 0 to 5 seconds. During this time span the output voltage and the current are consistent.

G. Fixed power from ac grid

For this case, solar irradiation is maintained constant at 1000W/m^2 and wind speed is maintained constant at 12m/s. The apparent load is maintained at 5220VA (5kW, 1500VAR). A disturbance is created at 2sec and DC Micro grid is removed from the system by using a breaker. Results for these changes are observed below.

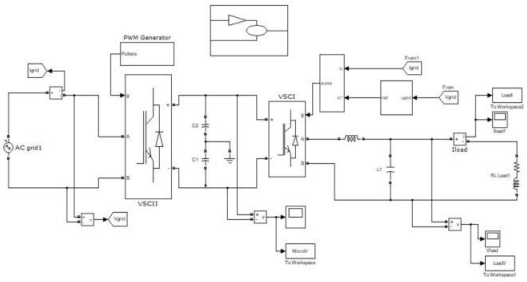

Fig. 41. Equivalent simulink model for fixed power from AC grid

For this case, simulation scheme is shown in Fig. 1. Equivalent simulink model for fixed power AC grid is shown in Fig. 41. Response for this case is seen in below Fig. 42 & Fig. 43. Response observed for 0 to 5sec.

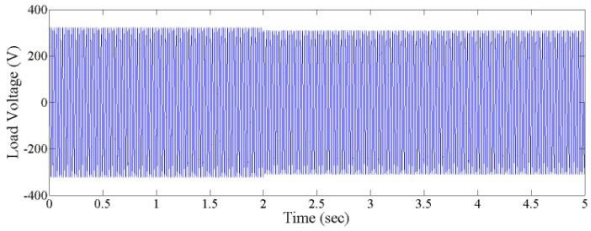

Fig. 42. Output Voltage for fixed power from AC grid

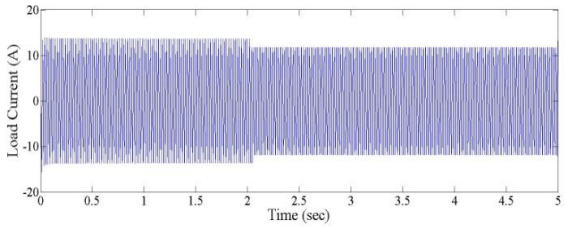

Fig. 43. Output Current for fixed power from AC grid

Observation:

Here DC micro grid is faulted with help of converter at 2 sec. The B2B converter is capable of managing the fault generated for 0.1 second at transient, after that transient died out. The output of the AC grid is only for 2 to 3 seconds duration. As observed, this response says that for this condition the output is present with no longer disturbances. Voltage sag can be observed a little. But at the end of 5 sec, rms voltage observed is 210V & rms current observed is 7.07A.

H. Fixed power from dc micro-grid

For this case, solar irradiation is maintained constant at 1000W/m^2 and wind speed is maintained constant at 12m/s. The apparent load is at 5220VA (5kW, 1500VAR). A disturbance is created at 2sec and utility grid is removed from the system by using a breaker. Results for these changes are observed below.

In this case, fault at utility side is shown in simulation scheme in Fig. 1. Equivalent simulink model for fixed power from DC micro grid shown in Fig. 44. The response of the system is shown in the Fig. 45 & Fig. 46. Response is observed for 0 to 5sec.

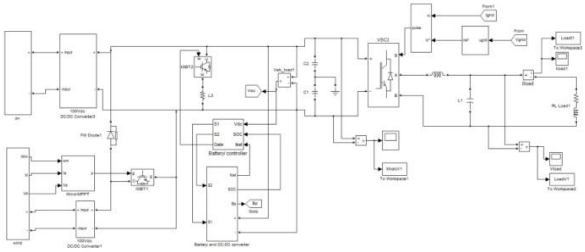

Fig. 44. Equivalent simulink model for fixed power from DC grid

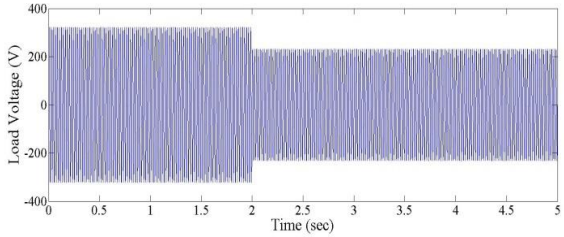

Fig. 45. Output Voltage for fixed power from DC micro grid

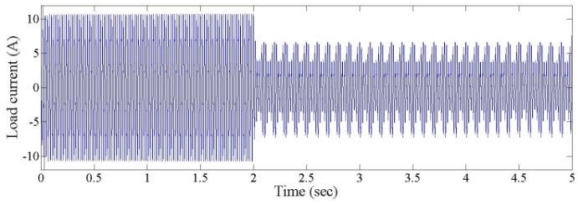

Fig. 46. Output Current for fixed power from DC micro grid

Observation:

The breaker is opened for respective fault time to establish fault at utility grid. Fault is induced between 2 and 3 seconds in this case. The voltage sag is observed for that moment, and the transient is present for 0.1 seconds after it dies. Then the DC micro grid's continuous output is observed in the response. Output via B2B is controlled by adjusting the pulse generator setting. Voltage sag observed here is noticeable. At 5 sec, rms voltage & rms current observed are 141V & 3.53A respectively.

5. Conclusions

- The connection is used to interconnect the micro-grid of the AC grid and DC. With effective and efficient transmission, power management is achieved. To achieve constant voltage output, the control strategy is used in the DC micro-grid. In the B2B converter, the enhanced control technique is retained under defective conditions.
- In faulty conditions, the system stays stable. Therefore, the load has no potential for injury. The voltage supply continues to the load with no interruption in the system at fault condition.
- In healthy conditions, voltage stability is enhanced. In this suggested method, power management is achieved efficiently.
- The suggested model also demonstrates that under all its operating conditions, the system retains a constant DC bus voltage. In each of these operating modes, the effects of the simulation are checked under the excess power mode and deficit power mode and the control of BESS. In addition, the value of the Battery Storage Energy Device is evident in the management and regulation of the DC microgrid.
- Eventually, the study shows that a DC microgrid is much simpler and offers more stability than an AC microgrid.
- This thesis reveals that,
- Management of power of both AC grid and DC micro grid can be done by using back to back converter there by increasing the reliability of load.
- Stability of DC and AC voltages.
- The stability of the system at fault-and-islanded condition

Scope for future work:

- There is the opportunity to integrate third party micro-grid to the AC grid from this back-to-back structure.
- Continuous supply of power to the load, whether faulty or stable. i.e., AC or DC micro grid can be operated in islanded operation.
- Stress on the utility grid can be minimized by the structure proposed.
- The requirement of DC micro-grid systems can be increased by increasing the usage of RES & by increasing number of micro sources like wind, PV, Battery. There by, fossil fuel dependency can be reduced.
- As isolated micro grids have reliability issues, the hybrid structure power system is necessity at distribution side can be done to increase the efficiency and reliability of overall system,
- DC micro-grid can operate independently or in part with AC grid by proposed scheme. The multiple ac-dc-ac conversion will be used to achieve power management scheme.

References

[1] M. H. J. Bollen and F. Hassan, “Integration of Distributed Generation in the Power System,” Wiley-IEEE Press, New York, 2011.

[2] R. Zamora and A. K. Srivastava, "Energy management and control algorithms for integration of energy storage within microgrid," *2014 IEEE 23rd International Symposium on Industrial Electronics (ISIE)*, 2014, pp. 1805-1810.

[3] L. Xiong, W. Peng, and P. Loh, “A hybrid AC/DC micro-grid,” in *Proc. IPEC 2010 Conf*., Oct. 27–29, 2010, pp. 746–751.

[4] R. Majumder, "A Hybrid Microgrid with DC Connection at Back to Back Converters," in *IEEE Transactions on Smart Grid*, vol. 5, no. 1, pp. 251-259, Jan. 2014.

[5] H. Mohsenian-Rad and A. Davoudi, "Towards Building an Optimal Demand Response Framework for DC Distribution Networks," in *IEEE Transactions on Smart Grid*, vol. 5, no. 5, pp. 2626-2634, Sept. 2014.

[6] F. Katiraei and M. R. Iravani, "Power Management Strategies for a Microgrid with Multiple Distributed Generation Units," in *IEEE Transactions on Power Systems*, vol. 21, no. 4, pp. 1821-1831, Nov. 2006.

[7] F. Katiraei and M. R. Iravani, “Power management strategies for a micro grid with multiple distributed generation units,” in *IEEE Trans. Power Syst.*, vol. 21, no. 4, pp. 1821–1831, Nov. 2006.

[8] M. Reza, D. Sudarmadi, F. A. Viawan, W. L. Kling and L. van der Sluis, "Dynamic Stability of Power Systems with Power Electronic Interfaced DG," *2006 IEEE PES Power Systems Conference and Exposition*, 2006, pp. 1423-1428.

[9] A. Ghazanfari, M. Hamzeh, H. Mokhtari, and H. Karimi, "Active power management of multihybrid fuelcell/supercapacitor power conversion system in a medium voltage micro grid," in *IEEE Trans. Smart Grid*, vol. 3, no. 4, pp. 1903–1910, Dec. 2012

[10] P. Loh, D. Li, Y. Chai, and F. Blaabjerg, "Autonomous operation of hybrid micro grid with AC and DC sub-grids," in *IEEE Trans. Power Electron*., vol. 28, no. 5, pp. 2214–2223, May 2013.

[11] P. C. PChao, W. D. Chen, and C. K. Chang, "Maximum power tracking of a generic photovoltaic system via a fuzzy controller and a two-stage DC–DC converter," in *Microsyst Technol*., vol. 18, pp. 1267–1281, 2012.

[12] M. Saleh, Y. Esa and A. A. Mohamed, "Communication-Based Control for DC Microgrids," in *IEEE Transactions on Smart Grid*, vol. 10, no. 2, pp. 2180-2195, March 2019.

[13] D. E. Olivares et al., "Trends in Microgrid Control," in *IEEE Transactions on Smart Grid*, vol. 5, no. 4, pp. 1905-1919, July 2014.

[14] D. Miao and J. Shen, "Comparative study on permanent magnet synchronous generator systems with various power conversion topologies," *4th International Conference on Power Engineering, Energy and Electrical Drives*, 2013, pp. 1738-1743.